

# Experimental determination of the charge/neutral branching ratio $\eta$ in the photoexcitation of $\pi$ -conjugated polymers by broadband ultrafast spectroscopy

C.-X. Sheng, M. Tong, S. Singh, and Z. V. Vardeny\*

*Physics Department, University of Utah, Salt Lake City, Utah 84112, USA*

(Received 27 May 2006; published 12 February 2007)

We demonstrate a long-sought reliable method for determining the important branching ratio  $\eta$  between photogenerated charged polarons and neutral excitons in  $\pi$ -conjugated polymer films and solutions, using femtosecond transient photomodulation spectroscopy with broad spectral range from 0.14 to 2.7 eV. We found that both excitons and polarons are instantaneously photogenerated, but  $\eta$  critically depends on the film nanomorphology, which ultimately controls the interchain coupling strength. We also found that a correlation exists within each polymer family between the obtained  $\eta$  value, photoluminescence quantum efficiency, and the transient polarization memory lifetime; where the interchain coupling strength in the film determines them all. We show that  $\eta$  varies from less than 1% in solutions and glassy films of poly(p-phenylene-vinylene) derivatives, where the polymer chains are relatively isolated; to more than 30% in ordered films that contain lamellae, such as regio-regular poly(3-hexyl-thiophene). Our results may serve for matching polymers to specific device applications, where polymers with large  $\eta$  values are good candidates for photodetector and photovoltaic applications, whereas those with small  $\eta$  values are more suitable for active layers in organic light emitting devices.

DOI: [10.1103/PhysRevB.75.085206](https://doi.org/10.1103/PhysRevB.75.085206)

PACS number(s): 78.47.+p, 71.35.Cc, 76.70.Hb, 78.45.+h

## I. INTRODUCTION

$\pi$ -conjugated polymers find applications in a range of devices such as organic light emitting diodes (OLEDs), field effect transistors, and solar cells.<sup>1</sup> It is not surprising therefore that the photoexcitations properties in these materials have been extensively studied by experiment and theory, especially since their applications may depend on the ratio  $\eta$  of charged (polarons) to neutral (excitons) photoexcitations following photon absorption. Specifically, if  $\eta$  is large, then solar cell and solid-state photodetector applications are in order; in contrast, for OLEDs it is preferable to use polymers with small  $\eta$ .<sup>1</sup> Photogeneration of polarons in  $\pi$ -conjugated polymer films with various nanomorphologies is thus of practical interest, especially since the traditional one-dimensional (1D) electronic properties of the polymer chain may be modified by the consequent interchain coupling.<sup>2</sup> Measuring primary polaron photogeneration in the femtosecond (fs) time domain is regarded as the most suitable method for determining  $\eta$ .<sup>3</sup> However, so far only limited spectral ranges have been studied with the aim of measuring  $\eta$  in polymer films and solutions.<sup>3–10</sup>

It is well known that the main polaron absorption band in  $\pi$ -conjugated polymers lies in the mid-IR spectral range,<sup>2,11</sup> which has not been studied by ultrafast spectroscopy since it is not easily accessible using femtosecond (fs) pulses. This may be the main reason that controversies in the obtained  $\eta$  values in polymer films and solutions have flourished in the last decade. For example, a variety of transient spectroscopic methods for measuring  $\eta$  have been used in pristine films of poly(phenylene-vinylene) [PPV] derivatives;<sup>3–10</sup> however, with large variation in the obtained  $\eta$  values that ranged between 0.1% and 10%, even in films cast from the same polymer solution.<sup>3,8</sup> Another reason for these unsettled  $\eta$  values may be that methods which have been successfully used to determine  $\eta$  in semiconductors, such as the transient mi-

crowave conductivity<sup>12</sup> and THz spectroscopy,<sup>8,9</sup> are suspect for using in polymers, since the charge polarons in these soft materials do not show obvious features in the far-IR spectral range.<sup>11</sup>

In this work we used the transient photomodulation (PM) spectroscopy with 150-fs time resolution within a broad spectral range from 0.14 to 2.7 eV, which also includes the polaron photoinduced absorption (PA) band in the mid-IR spectral range,<sup>2,11</sup> for determining  $\eta$  in various pristine polymer films and solutions. The main reason for the success of our unique method is that both exciton and polaron PA bands are simultaneously detected with our laser systems. Thus for obtaining a reliable  $\eta$  value we used the ratio of the polaron/exciton PA bands in the mid-IR range, where they are well separated, and readily measured with the same low power laser system. The obtained  $\eta$  values vary dramatically between  $\sim 0.5\%$  in PPV derivative solution and  $\sim 30\%$  in regio-regular (RR) poly(3-hexyl thiophene) [P3HT] films, depending on the polymer structure and film nanomorphology. Interestingly, we found that the  $\eta$  value in films of PPV derivatives crucially depends on the solvent used for film casting;  $\eta \sim 10\%$  when the films are cast from toluene solution, but  $\eta < 1\%$  if chloroform solution is used. We also found that the variation in the film  $\eta$  value within a polymer family echoes that of the photoluminescence (PL) quantum efficiency, and the lifetime of the exciton polarization memory transient decay. We conclude that all these optoelectronic parameters are in fact determined by the strength of the interchain coupling in the film.

## II. EXPERIMENT

For the polarized transient PM spectroscopy we used the fs two-color pump-probe correlation technique with two laser systems based on Ti:sapphire oscillator:<sup>13</sup> a low power (energy/pulse  $\sim 0.1$  nJ), high repetition rate ( $\sim 80$  MHz) la-

ser for the mid-IR spectral range; and a high power (energy/pulse  $\sim 10 \mu\text{J}$ ), low repetition rate ( $\sim 1 \text{ kHz}$ ) laser for the near-IR–visible spectral range. In both laser systems the excitation photon energy  $\hbar\omega$  was 3.2 eV. For the low intensity measurements we used an optical parametric oscillator (Opal, Spectra Physics) as a probe, which generates  $\hbar\omega(\text{probe})$  from 0.55 to 1.05 eV, and from 0.14 to 0.43 eV,<sup>13</sup> respectively. For the high intensity measurements, the white light supercontinuum was generated for  $\hbar\omega(\text{probe})$  ranging from 1.15 to 2.7 eV. The transient PM signal  $\Delta T/T(t)$  is the fractional change in transmission  $T$ , which is negative for PA and positive for photobleaching (PB) and stimulated emission (SE). The transient PM spectra from the two laser systems were normalized to each other in the near-IR–visible spectral range, for which  $\hbar\omega(\text{probe})$  from the low power laser system was frequency doubled. For the polarization memory decay related to the photogenerated excitons we measured  $\Delta T$  at the SE band, with pump and probe polarizations either parallel [ $\Delta T(\text{pa})$ ] or perpendicular [ $\Delta T(\text{pe})$ ] to each other; the transient polarization memory  $P(t)$  was then obtained using the relation  $P(t) = [\Delta T(\text{pa}) - \Delta T(\text{pe})] / [\Delta T(\text{pa}) + \Delta T(\text{pe})]$ .<sup>14</sup>

The PPV derivative polymers studied here were synthesized in our laboratory, and include PPV, 2-methoxy-5-(2'-ethylhexyloxy) PPV [MEH-PPV] of which backbone structure is given in Fig. 1(a), inset, and 2,5-diethyloxy PPV [DOO-PPV]. The films were drop-cast from dilute solutions of various solvents such as water for PPV, toluene, chloroform, and tetrahydrofuran (THF) for MEH-PPV, and toluene for DOO-PPV. The P3HT polymers with regio-regular (RR) and regio-random (RRa) orders were purchased from ADS Inc. For comparison with PM spectra in films of polymer-fullerene blends, we also prepared films from MEH-PPV mixed with 10%  $\text{C}_{60}$  in a dilute toluene solution.

### III. RESULTS AND DISCUSSION

In a strictly 1D chain model, a single charge carrier added onto the polymer chain forms a spin- $1/2$  polaron, with two allowed optical transitions,  $P_1$  and  $P_2$  below the optical gap [Fig. 1(b)].<sup>11</sup> These are the *most prominent characteristic signatures* of charged polarons, which we use here in determining  $\eta$ . There is also an associated photoinduced electro-absorption (EA) band close to the optical-absorption onset;<sup>15</sup> but very little polaron induced absorption in the microwave to THz spectral ranges.<sup>8,9,12</sup> In addition, because of the relatively strong electron-phonon coupling in  $\pi$ -conjugated polymers, the polaron excitation renormalizes the frequencies of the Raman-active amplitude modes,<sup>16</sup> which consequently borrow IR intensity from the electronic transitions. The small polaronic mass causes these IR-active vibrations (IRAV) to possess large oscillator strengths which are comparable to those of the electronic-related transitions<sup>16</sup> [see, for example,  $\nu_1$  and  $\nu_2$  in Fig. 2(b), inset]. Once the electron-hole interaction is added to the model Hamiltonian that describes the electronic states in  $\pi$ -conjugated polymers, then the excited states become excitonic in nature with alternating odd ( $B_u$ ) and even ( $A_g$ ) parity symmetry.<sup>17</sup> Within this model the lowest-lying singlet  $\pi$  exciton in PPV-like chains is the

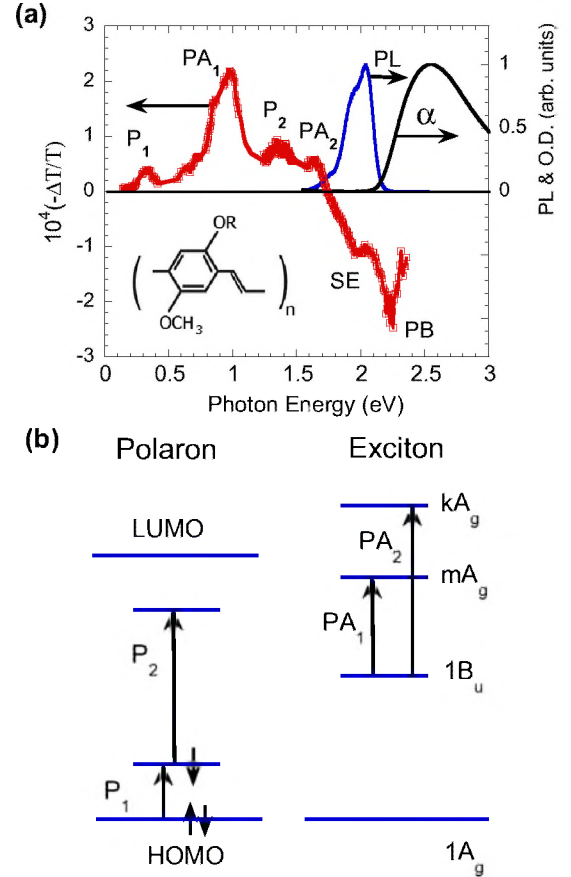


FIG. 1. (Color online) (a) The transient PM spectrum at  $t=0$  of pristine MEH-PPV film cast from toluene solution in the spectral range of 0.15–2.4 eV; the inset shows the polymer backbone structure. Various spectral bands are assigned;  $P_1$  and  $P_2$  are for polarons;  $PA_1$  and  $PA_2$  are for excitons; and SE and PB are stimulated emission and photobleaching of the absorption, respectively. The absorption and photoluminescence spectra are also shown for comparison. (b) The energy levels and optical transitions (schematically) of positively charged polaron, and singlet exciton in  $\pi$ -conjugated polymers within the exciton model (Refs. 7 and 17).  $1B_u$ ,  $mA_g$  and  $kA_g$  are odd and even parity exciton states in the neutral manifold, and HOMO (LUMO) is the highest (lowest) occupied (unoccupied) molecular orbital in the charge manifold.

$1B_u$ , which is strongly coupled to two excited  $A_g$  states, namely  $mA_g$  and  $kA_g$ . This produces two strong optical transitions  $PA_1$  and  $PA_2$  that characterize the photogenerated exciton in the polymer chain [Fig. 1(b)].<sup>7</sup> The PA bands  $P_1$  and  $P_2$  for polarons and  $PA_1$  and  $PA_2$  for excitons identify these photoexcitations in the transient PM spectrum.

#### MEH-PPV polymer films

Figure 1(a) shows the transient PM spectrum of a MEH-PPV film cast from toluene solution at “ $t=0$ ” (i.e., within 150 fs). It contains excitons with  $PA_1$  and  $PA_2$  bands at 0.95 and 1.6 eV, respectively, as well as polarons with  $P_1$  and  $P_2$  bands at 0.35 and 1.4 eV, respectively. In addition, there are also SE and PB bands. We measured [Fig. 2(a), inset]<sup>18,19</sup> that the polaron PA bands in the PM spectrum have slower

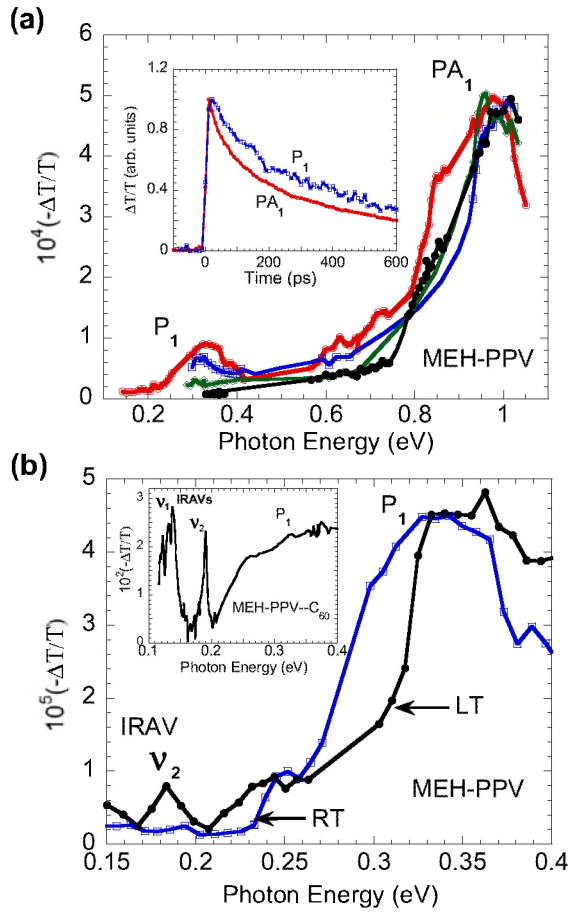


FIG. 2. (Color online) (a) Transient PM spectra at  $t=0$  in the spectral range of 0.14 to 1.05 eV of MEH-PPV films cast from toluene (red, empty circles), THF (blue, squares), and chloroform (green, diamonds), as well as a dilute toluene solution of the polymer (black, full circles). The bands  $P_1$  of polarons and  $PA_1$  of excitons are assigned. The inset shows the decay dynamics of the exciton and polaron bands. (b) The  $t=0$  transient PM spectra of MEH-PPV film cast from toluene solution in the mid-IR spectral range from 0.15–0.4 eV at 80 K (LT; black line, full circles) and room temperature (RT; blue line, empty squares). The bands  $P_1$  and IRAV  $\nu_2$  are assigned. The inset shows the PM spectrum of 10% C<sub>60</sub>-doped MEH-PPV film at 80 K in the same spectral range, where  $P_1$  and IRAV bands are assigned.

dynamics compared to those of the exciton PA bands, and the associated SE. This indicates that the two pairs of PA bands belong to different photogenerated species, namely excitons and polarons, respectively. Also at low temperatures the transient PM spectrum contains photoinduced IRAV that are correlated with the  $P_1$  band [Fig. 2(b)]; and this shows that the related photoexcitations are indeed charged.<sup>20</sup> In addition, the  $P_1$  band in the transient PM spectrum is similar to that in the steady-state PM spectrum of 10% polymer/C<sub>60</sub> blend [Fig. 2(b), inset] that is due to long-lived polarons.<sup>21</sup> We therefore conclude that the primary photoexcitations in MEH-PPV films are both excitons and polarons<sup>5,6,22</sup> that are generated instantaneously.

If we assume that singlet exciton and polaron excitations have roughly the same optical cross sections due to their

TABLE I. Branching ratio  $\eta$  of charged (polarons) to neutral (excitons) photoexcitations polarization memory decay time and PL quantum efficiency in several  $\pi$ -conjugated polymer films and solution.

Samples	Solvent	$\eta$ (%)	Polarization memory lifetime (ps)	PL quantum efficiency (%)
MEH-PPV Films	Toluene	10	2	15
	THF	8	3	17
	Chloroform	1	54	20
MEH-PPV Solution	Toluene	0.5	260	35
PPV	Water	10	22	26
DOO-PPV	Toluene	1	57	19
RR-P3HT	Toluene	30	93	1
RRa-P3HT	Toluene	1	120	10

similar one-dimensional (1D)  $\pi$ -electron character, and wave-function extent,<sup>11,13</sup> then from the broad PM spectrum at  $t=0$  we are able to estimate the photogeneration branching ratio  $\eta$  of polarons to excitons from the relative strength of their corresponding PA bands. From the PM spectrum of Fig. 1(a) we thus estimate  $\eta \approx 10\%$  for MEH-PPV film cast from toluene solution, in agreement with Ref. 3 but in sharp disagreement with Ref. 9. Actually we may conveniently estimate  $\eta$  from the intensity ratio  $P_1/PA_1$  in the mid-IR spectral range, using the low intensity laser system alone [see Fig. 2(a)], thus avoiding the complex recombination processes typical of high intensity laser systems.<sup>5</sup> Also knowing the precise optical cross-section ratio between excitons and polarons is not crucial in comparing the  $\eta$  value within the same polymer family that may have different film nanomorphologies depending on the film casting method and solvent used.

We used the PA intensity ratio in the mid-IR method to estimate the  $\eta$  value in other MEH-PPV films and solutions (Table I). Figure 2(a) compares the transient PM spectrum at  $t=0$  in the mid-IR spectral range of three MEH-PPV films cast from solutions of toluene, THF, and chloroform, respectively, as well as a dilute solution of MEH-PPV in toluene. We found that in chloroform-based film  $\eta \sim 1\%$ ; but  $\eta < 0.5\%$  in dilute toluene solution; a value smaller to that obtained in Ref. 10. The variations in  $\eta$  value among the different MEH-PPV films and solutions can be tracked back to their nanomorphologies. It was deduced from the variation in the PL quantum efficiency, as well as various nanoprobe images, that the degree of interchain interaction in MEH-PPV films sensitively depends on the solvent used in casting the film.<sup>23,24</sup> Using an integrated sphere for collecting the total PL emission coming from the photoexcited film, we indeed measured that films cast from toluene solutions have lower PL emission quantum efficiency (QE  $\sim 15\%$ ) than those cast from THF (QE  $\sim 17\%$ ) and chloroform (QE  $\sim 20\%$ ) (Table I), presumably because the polymer chains in the former film have more favorable nanomorphology for interchain interaction.<sup>23,24</sup>

For completeness we also measured the exciton polarization memory transient decay  $P(t)$  within the SE band of vari-



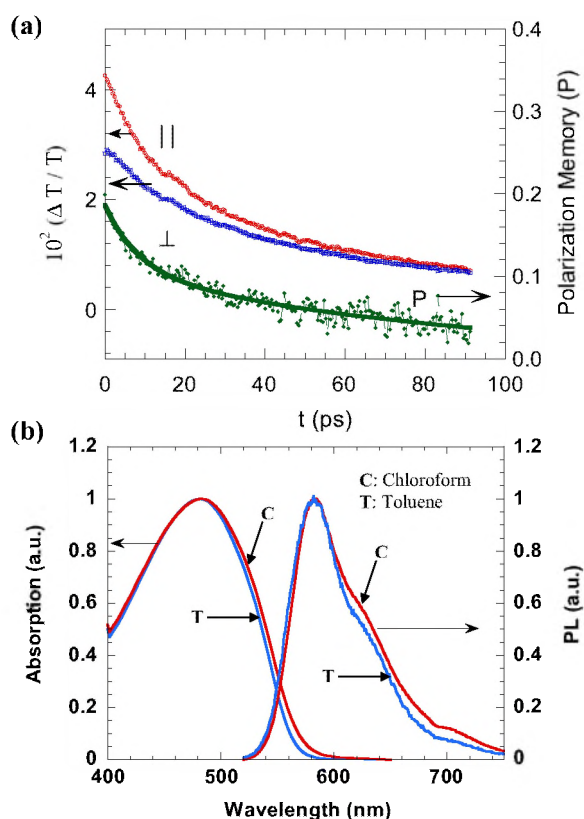


FIG. 3. (Color online) (a) The ps decay dynamics of  $\Delta T$  parallel (red line),  $\Delta T$  perpendicular (blue line) (left axis); and the resulting polarization memory,  $P(t)$  at the SE band of DOO-PPV film ( $\sim 2.0$  eV) (green line; right axis); that includes a zero level shift. (b) The room-temperature absorption and PL spectra of MEH-PPV films cast from toluene (blue line) and chloroform (red line).

ous DOO-PPV films [Fig. 3(a)], with the assumption that faster  $P(t)$  decay indicates stronger interchain coupling leading to a more mobile exciton.<sup>7</sup> A polarization memory value,  $P \sim 0.2$ , is initially formed in the polymer films because polymer chains with orientation parallel to the pump beam polarization are preferentially excited.<sup>7,14</sup>  $P(t)$  decays, however, due to exciton diffusion among the polymer chains in the film that randomize their vector dipole moment direction. We found that  $P(t)$  lifetime  $\tau$  is  $\sim 2$  ps in MEH-PPV films cast from toluene solution having large  $\eta$  value, whereas  $\tau \sim 54$  ps in chloroform based films that show small  $\eta$  value (Table I). The change in  $\tau$  value between MEH-PPV films cast from toluene and chloroform solution is amazing, since very little change is observed in their PL and absorption spectra [see Fig. 3(b)]. Although there is a slight blueshift in the PL and absorption spectra of films cast from toluene solution, this cannot explain the large difference in the obtained  $\eta$  and  $\tau$  values of these films. We thus conjecture that interchain coupling is more favorable in MEH-PPV films cast from toluene solution leading to more mobile exciton, and this explains their faster polarization memory decay. In polymer solution, where the PL QE is the highest, we indeed obtained the lowest  $\eta$  value, and longest  $\tau$  value, indicating much weaker (or lack of) interchain coupling. We thus conclude that the polaron photogeneration efficiency in MEH-

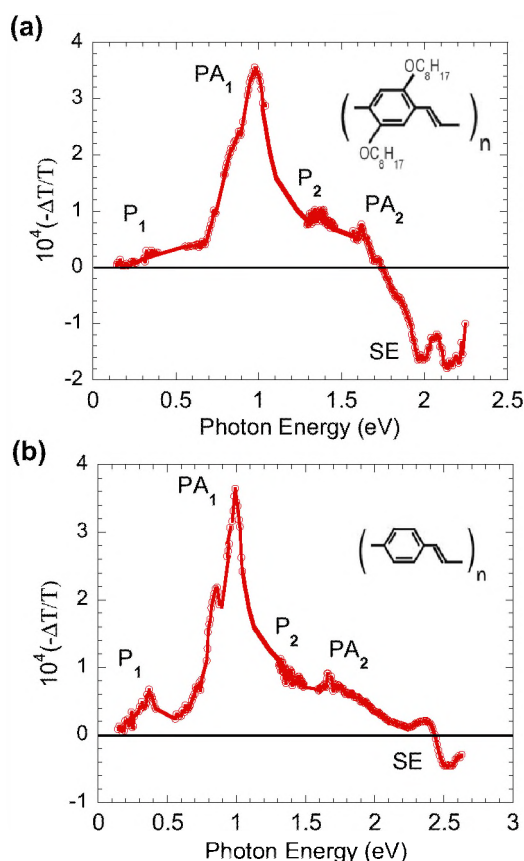


FIG. 4. (Color online) Same as in Fig. 1(a) but for films of DOO-PPV polymer (a) and PPV polymer (b). The polymer repeat units are given in the insets.

PPV depends on the film nanomorphology, which also determines the interchain coupling strength; and consequently also the PL efficiency and exciton polarization memory decay dynamics.

#### DOO-PPV and PPV polymer films

Figure 4 shows the broadband transient PM spectrum of two other PPV-based polymer films, namely DOO-PPV cast from toluene solution [repeat unit shown Fig. 4(a), inset], and unsubstituted PPV cast from water solution of a precursor compound [repeat unit shown in Fig. 4(b), inset]. In fact the PM spectra for these polymers (Fig. 4) are very similar to that shown in Fig. 1(a) for MEH-PPV.<sup>18,25</sup> Similarly, each PM spectrum contains two pairs of PA bands, namely  $PA_1$  and  $PA_2$  for photoexcited excitons, and  $P_1$  and  $P_2$  for photogenerated polarons; also the exciton PA bands are accompanied by a SE band in the visible spectral range. We note, however, that the  $P_1$  band for polarons in PPV is much stronger than that in DOO-PPV; and this indicates a larger  $\eta$  value in PPV films. Indeed from the  $P_1/PA_1$  intensity ratio in the mid-IR spectral range we estimate  $\eta \sim 10\%$  in PPV, whereas  $\eta < 1\%$  in DOO-PPV (Table I). In agreement with the role of interchain coupling strength in determining the  $\eta$  value, it is known that DOO-PPV films have mainly isolated polymer chains that result in weak interchain interaction,<sup>7</sup> whereas

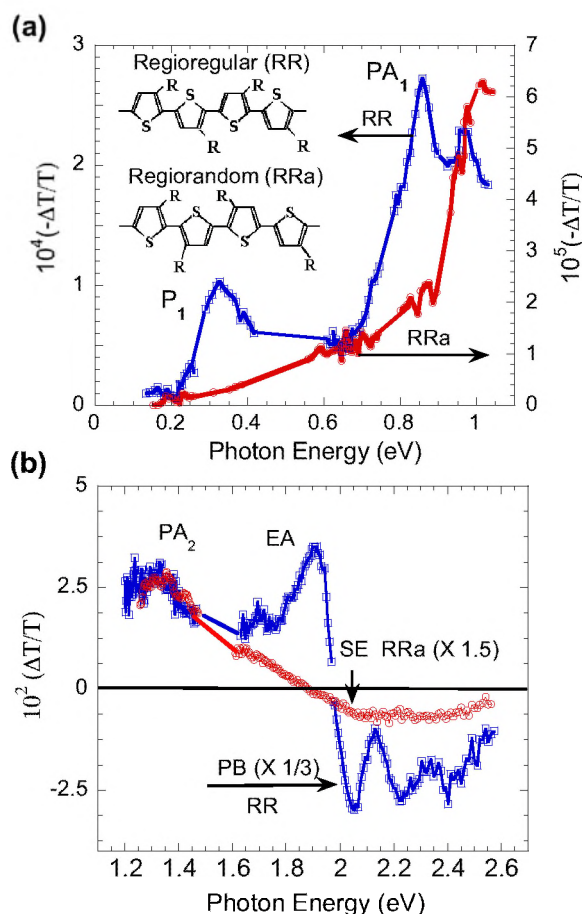


FIG. 5. (Color online) Transient PM spectra at  $t=0$  of RR-P3HT (blue, squares) and RRa-P3HT (red, circles) films in (a) mid IR, and (b) visible spectral range. The polymers backbone structures are shown in the inset to (a), where the different regio-orders are emphasized. The polaron bands  $P_1$  and  $P_2$  and associated photoinduced electroabsorption EA are assigned; along with the exciton bands  $PA_1$ ,  $PA_2$ , SE, and PB.

PPV films contain polymer chains with preferred orientation for increased interchain interaction.<sup>25</sup> It is worth noting that  $\eta$  and  $\tau$  values, and PL QE of DOO-PPV are similar to that of MEH-PPV films cast from chloroform solution (Table I), and this indicates that the polymer chains in these two films have very similar nanomorphologies. The obtained  $\eta$  values thus shows that the film nanomorphology is crucial in determining the  $\eta$  value, except that for different polymers in the same family it is determined by the polymer repeat unit rather than the solvent used.

### P3HT polymers

We extended our measurements to also include RR- and RRa-P3HT polymer films, which are perfect examples that show how the film nanomorphology influences, or even dominates the charge photogeneration QE in polymer films. RR-P3HT and RRa-P3HT polymers share the same backbone repeat unit [see Fig. 5(a), inset], but differ in their side groups arrangement. Nevertheless, their PL efficiencies differ dramatically; the PL QE is  $<1\%$ , and  $10\%$  for RR- and

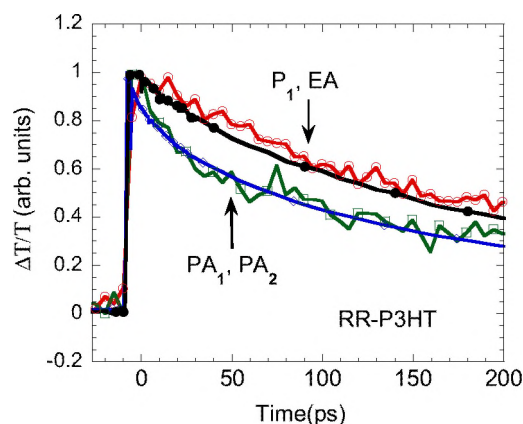


FIG. 6. (Color online) Transient ps decay dynamics in RR-P3HT film of the polaron bands:  $P_1$  (red line, empty circles) and EA (black line, full circles) compared to those of the exciton bands:  $PA_1$  (green line, squares) and  $PA_2$  (blue line, diamonds).

RRa-P3HT films, respectively<sup>21</sup> (Table I). The high carrier mobility and lack of strong PL has made RR-P3HT an ideal polymer candidate for use in polymer-fullerene organic solar cells based on bulk heterojunctions.<sup>26</sup> The reason for the differences in their physical properties is that self-organization of RR-P3HT chains results in formation of lamellae structure perpendicular to the film substrate; such 2D lamellae sheets have strong interchain interaction due to the short interchain interlayer distance of the order of  $3.8 \text{ \AA}$ .<sup>2</sup> On the contrary, RRa-P3HT films form lamellae to a lesser degree, and thus the normal, isolated chainlike morphology governs its optoelectronic properties.<sup>2</sup>

We compare in Fig. 5 the transient PM spectra in the mid-IR [Fig. 5(a)] and visible [Fig. 5(b)] spectral ranges of RR-P3HT and RRa-P3HT films at  $t=0$ . In the PM spectra of RR-P3HT it is seen that the polaron  $P_1$  band in the mid-IR ( $\sim 0.35 \text{ eV}$ ) is relatively strong; and is accompanied in the visible range by a strong photoinduced EA modulation,<sup>15</sup> with phonon sideband peaks at  $\sim 1.9$ ,  $2.1$ , and  $2.3 \text{ eV}$ , respectively. In addition, no SE band associated with excitons is seen in the PM spectrum [Fig. 5(b)]. The decay dynamics of the various PA bands in RR-P3HT are shown in Fig. 6, and clearly separate polaron bands ( $P_1$  and EA) with slower dynamics, from those related to excitons ( $PA_1$  and  $PA_2$ ) that decay faster. In contrast, the  $P_1$  band in RRa-P3HT is negligibly small [Fig. 5(a)], and there is no photoinduced EA band [Fig. 5(b)]; instead, a prominent SE band appears in the visible range. These spectral features are consistent with low polaron photogeneration quantum efficiency, in agreement with the chainlike nanomorphology of this polymer film. Using our method of  $P_1/PA_1$  intensity ratio in the mid-IR to determining  $\eta$  we found that  $\eta \sim 30\%$  in RR-P3HT films, which is higher than estimated in Ref. 6. We note that this is the highest  $\eta$  value that we have obtained so far in pristine polymer films. In contrast, the upper limit of  $\eta$  in RRa-P3HT is  $\sim 1\%$ , similar to that in glassy films of PPV derivatives (Table I). Also its PL efficiency and  $\tau$  value are higher than those in the RR-P3HT counterpart; in agreement with the correlation found above between  $\eta$  and  $\tau$  values and PL QE in PPV derivatives (Table I).

The vastly different  $\eta$  values obtained in the two regio-ordered P3HT polymer films is consistent with the measured maximum power conversion efficiency (PCE) of solar cells based on blends of these polymers with fullerene derivatives as acceptors. Whereas the maximum PCE of RR-P3HT/fullerene solar cells is  $\sim 5\%$ ,<sup>26</sup> and crucially depends on the amount of RR order in the polymer chain, PCE of cells based on RRa-P3HT/fullerene blends is much smaller.<sup>27</sup> Our results indicate therefore that the pristine film nanomorphology also plays an important role in determining the photoinduced charge separation and polaron mobility in polymer-fullerene blends.

#### Comparison with other measurement techniques

The  $\eta$  values obtained here are much larger than those obtained using microwave conductivity<sup>12</sup> and THz spectroscopy.<sup>8,9</sup> It is well known in the field of  $\pi$ -conjugated polymers that charge carriers are accommodated upon doping in the form of polarons. The optical conductivity (or optical absorption) spectrum shows the formation of two localized states in the highest occupied molecular orbital–lowest unoccupied molecular orbital gap of the polymer that lead to two absorption bands below the optical gap.<sup>11</sup> This is *in contrast* to the impurity absorption band and Drude-type conductivity spectrum that are formed upon doping in more conventional semiconductors. In addition to the two doping induced absorption bands, the spectrum of doped polymers also contains polaron-related IRAV down to  $\sim 400\text{ cm}^{-1}$ ,<sup>16</sup> *but there is little contribution in the THz and microwave spectral ranges.* The reason for this unusual situation is that the electrical conductivity of  $\pi$ -conjugated polymers is relatively small, because the contribution due to mobile free carriers is usually quite small.<sup>28</sup> On the contrary, hopping and variable range hopping have been routinely recognized as the main mechanism of carrier transport in these disordered materials.<sup>29</sup> The hopping mechanism leads to very small optical conductivity at low frequencies including microwave and THz spectral ranges.<sup>30</sup> Therefore it is not clear whether the use of spectroscopic tools in these two spectral ranges, which have been routinely used in inorganic semiconductors, is suitable for studying carrier photogeneration and transport in  $\pi$ -conjugated polymers. No wonder therefore that  $\eta$ -value estimates using these two techniques showed very small polaron photogeneration QE in MEH-PPV, of order  $10^{-3}$  in films and  $10^{-5}$  in solutions.<sup>9</sup> Whereas we conclude in our present work a branching ratio of  $\sim 10\%$  in films of this same polymer, and  $1\%$  in solution; which constitutes a factor

of  $\sim 100$  difference between our findings and those in the previous work.<sup>9</sup> Moreover, using the microwave conductivity technique,  $\eta \sim 2\%$  was obtained in RR-P3HT films,<sup>12</sup> whereas we conclude a branching ratio of  $\sim 30\%$  in the same polymer. In general, our polaron QE estimates are closer to  $\eta$  values obtained via ultrafast transient photoconductivity<sup>31</sup> and photoinduced IRAV (Ref. 3) previously measured in polymer films, except that in our technique both polarons and excitons are simultaneously measured.

#### IV. CONCLUSION

We measured the ultrafast transient PM spectra within a broad spectral range from 0.14 to 2.7 eV, polarization memory decay, and PL efficiency in various pristine PPV derivative films cast from different solvents, and P3HT films with two regio-regular orders. Both excitons and polarons are instantaneously photogenerated in these films. We found that the polaron photogeneration QE  $\eta$  ranges from less than  $1\%$  in most films of PPV derivatives (depending on the solvent used) to  $\sim 30\%$  in films of RR-P3HT, as summarized in Table I. We also found that the  $\eta$  value in films is correlated within the same polymer family to the PL QE, and transient polarization memory lifetime  $\tau$ . The PL efficiency is lower and  $\tau$  is shorter in films showing higher  $\eta$  values. This correlation shows that all three optoelectronic characteristic parameters sensitively depend on the film nanomorphology, which also determines the underlying strength of the interchain interaction. We thus conclude that in films of strong interchain interaction the  $\eta$  value is higher, PL QE is lower, and exciton (and carrier) mobility is higher. A perfect example of this correlation is obtained RR-P3HT polymer films.

Having established a reliable method for measuring  $\eta$  value in polymer films, we may now proceed in using this method for measuring  $\eta$  in a variety of interesting ultrafast transient processes such as the photoinduced charge transfer in polymer-fullerene blends, photoinduced charge separation under the influence of a strong external electric field in OLED, and OLED degradation.

#### ACKNOWLEDGMENTS

We thank L. Wojcik and M. Delong for the polymer preparation, and R. Polson for help with the ultrafast measurements. The transient optical measurements in the visible range were performed at the John Dixon Laser Institute. This work was supported in part by U.S. DOE Grant No. FG-04ER46109. The University of Utah support for the Laser Institute is greatly appreciated.

\*Author to whom correspondence should be addressed. Email address: val@physics.utah.edu

<sup>1</sup>G. Malliaras and R. Friend, *Phys. Today* **58**, 53 (2005).

<sup>2</sup>R. Österbacka, C. P. An, X. M. Jiang, and Z. V. Vardeny, *Science* **287**, 839 (2000).

<sup>3</sup>P. B. Miranda, D. Moses, and A. J. Heeger, *Phys. Rev. B* **64**, 081201(R) (2001).

<sup>4</sup>C. Gadermaier, G. Cerullo, G. Sansone, G. Leising, U. Scherf, and G. Lanzani, *Phys. Rev. Lett.* **89**, 117402 (2002).

<sup>5</sup>C. Silva, A. S. Dhoot, D. M. Russell, M. A. Stevens, A. C. Arias, J. D. MacKenzie, N. C. Greenham, R. H. Friend, S. Setayesh, and K. Müllen, *Phys. Rev. B* **64**, 125211 (2001).

<sup>6</sup>A. Ruseckas, M. Theander, M. R. Andersson, M. Svensson, M. Prato, O. Inganäs, and V. Sundström, *Chem. Phys. Lett.* **322**,



- 136 (2000).
- <sup>7</sup>S. V. Frolov, Z. Bao, M. Wohlgenannt, and Z. V. Vardeny, *Phys. Rev. Lett.* **85**, 2196 (2000); *Phys. Rev. B* **65**, 205209 (2001).
  - <sup>8</sup>E. Hendry, M. Koeberg, J. M. Schins, L. D. A. Siebbeles, and M. Bonn, *Phys. Rev. B* **70**, 033202 (2004).
  - <sup>9</sup>E. Hendry, M. Koeberg, J. M. Schins, H. K. Nienhuys, V. Sundström, L. D. A. Siebbeles, and M. Bonn, *Phys. Rev. B* **71**, 125201 (2005).
  - <sup>10</sup>P. B. Miranda, D. Moses, and A. J. Heeger, *Phys. Rev. B* **70**, 085212 (2004).
  - <sup>11</sup>K. Fesser, A. R. Bishop, and D. K. Campbell, *Phys. Rev. B* **27**, 4804 (1983).
  - <sup>12</sup>G. Dicker, M. P. de Haas, L. D. A. Siebbeles, and J. M. Warman, *Phys. Rev. B* **70**, 045203 (2004).
  - <sup>13</sup>H. Zhao, S. Mazumdar, C.-X. Sheng, M. Tong, and Z. V. Vardeny, *Phys. Rev. B* **73**, 075403 (2006).
  - <sup>14</sup>C. X. Sheng, Z. V. Vardeny, A. B. Dalton, and R. H. Baughman, *Phys. Rev. B* **71**, 125427 (2005).
  - <sup>15</sup>J. Cabanillas-Gonzales, T. Virgili, A. Gambetta, G. Lanzani, T. D. Anthopoulos, and D. M. de Leeuw, *Phys. Rev. Lett.* **96**, 106601 (2006).
  - <sup>16</sup>E. Ehrenfreund, Z. Vardeny, O. Brafman, and B. Horovitz, *Phys. Rev. B* **36**, 1535 (1987).
  - <sup>17</sup>S. N. Dixit, D. Guo, and S. Mazumdar, *Phys. Rev. B* **43**, 6781 (1991).
  - <sup>18</sup>S. V. Frolov, P. A. Lane, M. Ozaki, K. Yoshino, and Z. V. Vardeny, *Chem. Phys. Lett.* **286**, 21 (1998).
  - <sup>19</sup>C.-X. Sheng, Ph.D. thesis, University of Utah, 2005.
  - <sup>20</sup>The IRAV in the fs PM spectrum appear weaker than in the cw spectrum [Fig. 2(b), inset] because of the typical poorer spectral resolution (Ref. 3) caused by the short pulse duration. The reason that the IRAV in pristine MEH-PPV films are stronger at low temperature is not clear at the present time.
  - <sup>21</sup>N. S. Sariciftci, L. Smilowitz, A. J. Heeger, and F. Wudl, *Science* **258**, 1474 (1992).
  - <sup>22</sup>O. J. Korovyanko, R. Österbacka, X. M. Jiang, Z. V. Vardeny, and R. A. J. Janssen, *Phys. Rev. B* **64**, 235122 (2001).
  - <sup>23</sup>L. Rothberg, *Proceedings of the International School of Physics "Enrico Fermi" Course CXLIX*, edited by V. M. Agranovich and G. C. La Rocca (IOS, Amsterdam, 2002), p. 299.
  - <sup>24</sup>B. J. Schwartz, *Annu. Rev. Phys. Chem.* **54**, 141 (2003).
  - <sup>25</sup>R. Österbacka, M. Wohlgenannt, M. Shkunov, D. Chinn, and Z. V. Vardeny, *J. Chem. Phys.* **118**, 8905 (2003).
  - <sup>26</sup>W. Ma, C. Y. Yang, X. Gong, K. Lee, and A. J. Heeger, *Adv. Funct. Mater.* **15**, 1617 (2005).
  - <sup>27</sup>Y. Kim, S. Cook, S. M. Tuladhar, S. A. Choulis, J. Nelson, J. R. Durrant, D. D. C. Bradley, M. Giles, I. McCulloch, C.-S. Ha, and M. Ree, *Nat. Mater.* **5**, 197 (2006).
  - <sup>28</sup>K. Lee, S. Cho, S. H. Park, A. J. Heeger, C.-W. Lee, and S.-H. Lee, *Nature (London)* **441**, 65 (2006), and references therein.
  - <sup>29</sup>R. S. Kohlman, J. Joo, and A. Epstein, in *Physical Properties of Polymers Handbook*, edited by J. E. Mark (AIP, Woodbury, NY, 1996), p. 453.
  - <sup>30</sup>T.-I. Jeon, D. Grischkowsky, A. K. Mukherjee, and R. Menon, *Appl. Phys. Lett.* **79**, 4142 (2001).
  - <sup>31</sup>C. H. Lee, G. Yu, D. Moses, and A. J. Heeger, *Phys. Rev. B* **49**, 2396 (1994).